Fourth International
Dam World Conference
PORTUGAL • LISBON • LNEC

DISCONTINUOUS HYDROMECHANICAL MODELLING OF CONCRETE DAM FOUNDATIONS

Gonçalo Freitas	M. Luísa B. Farinha[1]	Nuno M. Azevedo
FCT/UNL	LNEC	LNEC

João R. Almeida	Magda Sá	Noemi S. Leitão
FCT/UNL	FCT/UNL	LNEC

ABSTRACT

The analysis of the hydromechanical behaviour of concrete dam foundations requires coupled models which account for the role of deformation in fluid flow and the stability of the rock mass. In this study the hydromechanical analysis is performed by means of an explicit time stepping small displacement algorithm, Parmac3D-Fflow, based on a discrete representation of the discontinuities. In order to evaluate the practical importance of stress-sensitive fluid flow in rock mass discontinuities a case study is presented of an arch-gravity dam, 83 m high. Especial attention is given to boundary conditions, drainage system simulation and sets of mechanical and hydraulic parameters that may control flow and stress behavior.

This paper presents the results of the application of a 3D discontinuum hydromechanical model for the analysis of the behaviour of the dam foundation. In this hydromechanical model the hydraulic behaviour is simulated assuming that seepage takes place along channels located at the edges of the triangular interface elements which simulate the various discontinuities. In the study presented here the main emphasis is on the simulation of the drainage system and on the results of sliding stability analysis. Conclusions are drawn regarding the safety factors obtained using the traditional method of strength reduction and other methods in which the hydrostatic load is gradually increased.

Keywords: Concrete dams, Rock foundations, Hydromechanical behaviour, Numerical modelling, Failure analysis

[1] lbraga@lnec.pt, Portugal

1. INTRODUCTION

Numerical simulation of the hydromechanical behaviour of concrete dam foundations requires the use of numerical models that allow not only coupled analysis of both the rock mass mechanical behaviour and hydraulic behaviour but also adequate simulation of the foundation discontinuities and of the grout and drainage systems installed in the dam foundations [1,2].

Three-dimensional (3D) models are essential for arch dam foundation analysis and for gravity dams in which the dam height is variable along its axis or the geotechnical conditions are not uniform [3]. However, for 3D analysis, no discontinuous numerical tools are available that can solve in an integrated manner the hydromechanical coupled analysis and the subsequent stability assessment for static and seismic loads [4]. Traditionally, water pressures commonly used in concrete dam design are considered and imposed at the dam foundation discontinuities. A more realistic water pressure pattern may be obtained using a continuum based foundation model to perform hydraulic analysis [5] and the water pressures obtained can be taken into account in a discontinuum mechanical model, which is then used for stability analysis [1]. This justifies the need to develop robust 3D models, as the one used in this study, specifically designed to the analysis of dam foundations and capable of handling the coupled hydro-mechanical behaviour in an integrated manner.

This paper presents the results of the application of the 3D computational module Parmac3D-Fflow in the hydromechanical analysis of an arch-gravity dam. This computational module is based on interface finite elements and is an extension to 3D of a 2D model presented by Monteiro Azevedo and Farinha [6, 7] which has been validated [8] and used in previous studies [9, 10]. In the study presented herein, the main emphasis is on the simulation of the drainage system and on the results of sliding stability analysis using either the strength reduction method or an increase in hydrostatic loads.

2. DISCONTINUUM HYDROMECHANICAL MODEL

2.1. Mechanical model

The 3D discontinuum hydromechanical model used in this study is part of the Parmac3D-Fflow computational model, initially developed for concrete fracture analysis [11], which has been used for both static and dynamic analysis of the behaviour of concrete dams. In this computational model, the domain, which includes both the rock mass foundation and the dam, is divided into a group of blocks and it is necessary to ensure that the interaction between the various blocks is always face-to-face. The contact surfaces between adjacent blocks are fully compatible and these interfaces can slip and separate. Each model block is divided into tetrahedral elements, in order to simulate material deformability. The interaction between tetrahedral elements is face-to-face, and thus the interface elements are triangular elements. In these interface elements, the integration points coincide with nodal points.

2.2. Hydraulic model

The hydraulic model is built on the mechanical model, as explained in detail in [8], and both models are fully compatible. Figure 1 shows the two different hydraulic approaches that can be used. The first approach, shown in Figure 1a), is a 2D continuum seepage model, with triangular interface elements. This 2D hydraulic formulation is finite element based and was proposed by Yan and Zheng in 2017 [12]. The second approach, shown in Figure 1b), is a 1D seepage model, in which it is assumed that seepage takes place along channels located at the edges of the triangular interface elements which simulate the various discontinuities. This is an extension to 3D of the 2D model presented by Monteiro Azevedo and Farinha in 2015 [6, 7], which is based on a simpler but numerically more robust unidirectional flow formulation. It must be highlighted that for both hydraulic approaches there is a perfect compatibility between the mechanical and the hydraulic parts of model.

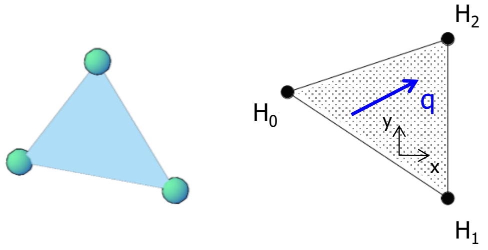

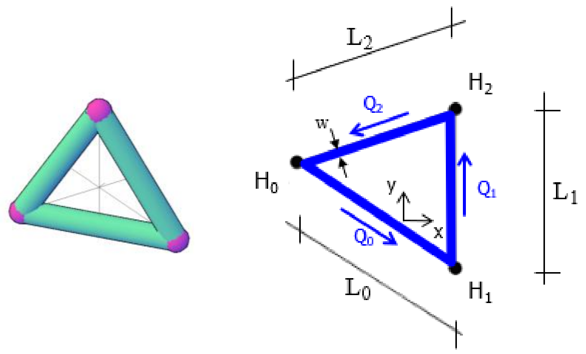

a) Triangular interface elements (adapted from [12])

b) Channels located at the edges of the triangular elements (adapted from [6, 7])

Fig. 1 – Triangular interface elements and seepage channels located at the edges of the triangular elements

The model which uses triangular interface elements to simulate the different discontinuities allows the 3D hydraulic and hydromechanical behaviour of jointed rock masses to be accurately simulated, because it is closer to reality. However, the model in which it is assumed that seepage takes place along channels is computationally simpler and widely used in practice. It can also be used to simulate unconfined groundwater steady state flows, i.e. flows bounded above by a phreatic surface, in the complex discontinuity networks that exist in rock masses. In addition, it presents a more robust solution that may be used in other type of problems, namely discrete particle analyses to simulate hydraulic fracturing.

Figure 1b) shows the hydraulic super nodes and the unidirectional seepage channels, called pseudo seepage channels, located on the edges of the triangular hydraulic interfaces. For the pseudo seepage channels located at the edges of the associated triangular interface, a pseudo width is calculated in such a way that the total area of the pseudo seepage channels is equal to the area of the hydraulic interface:

$$(L_0 + L_1 + L_2)\, w = \mathrm{A} \tag{1}$$

where L = length of each edge of the triangular interface; w = pseudo width, that mustbe calculated for each triangular interface element; and A = area of the triangular interface element.

Studies carried out by Sá [9] led to the conclusion that both hydraulic approaches are valid, but in order to obtain the same discharge with both models it is necessary to apply a multiplicative factor λ to the pseudo width. This factor needsto be calculated for each case, but its value is usually around 2.

2.3. Hydromechanical model

The calculation cycle of the hydromechanical model, shown in Figure 2, evolves over time through the interaction between the mechanical and the hydraulic domains, in a simple and sequential coupling. At each timestep there are three phases: i) firstly, the hydraulic apertures are calculated taking into account the normal displacements of the discontinuities calculated with the mechanical model; ii) secondly, water pressures are calculated in the hydraulic model; and iii) finally, these water pressures are transferred to the mechanical model as the effective stresses and the new mechanical apertures are calculated.

In Parmac3D-Fflow there is a perfect superimposition between both the mechanical and hydraulic models (the nodal points of the mechanical model are at the same position as the nodal points of the hydraulic model), which makes it easier to define boundary conditions and optimises transfer of informationbetween the two domains.

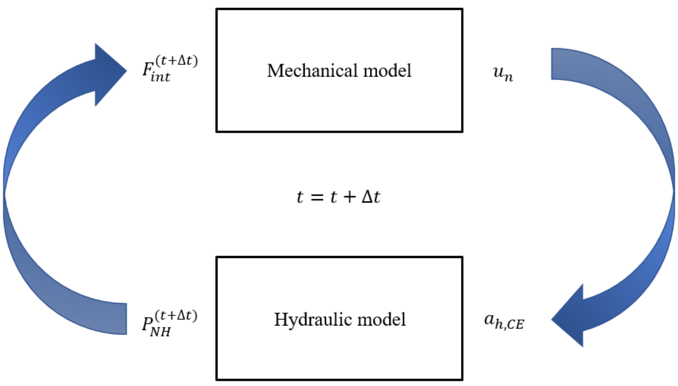

Fig. 2 – Calculation cycle of the hydromechanical model

3. NUMERICAL MODELLING OF AN ARCH-GRAVITY DAM

3.1. Ribeiradio dam

The geometry of Ribeiradio dam (Figure 3) was used as a basis to develop this study. It is an arch-gravity dam, located on the river Vouga, in Portugal, constructed for energy production, water supply and flood control. It has a maximum height of 83 m and a total length between the abutments of 265 m. The foundation consists of granite. For foundation seepage control, grout and drainage curtains were installed from the foundation gallery of the dam.

Fig. 3 – Downstream view of Ribeiradio dam

3.2. Model description

Figure 4 shows the 3D global model of Ribeiradio dam [13]. The concrete part of the mechanical model, with 20-node hexahedral elements, has 1119 blocks, 4600 triangular interfaces and 10872 nodal points. The foundation part of the mechanical modelis divided into 1584 hexahedral blocks, and the dam/foundation interface has 920 triangular interface elements, with 10124 nodal points.

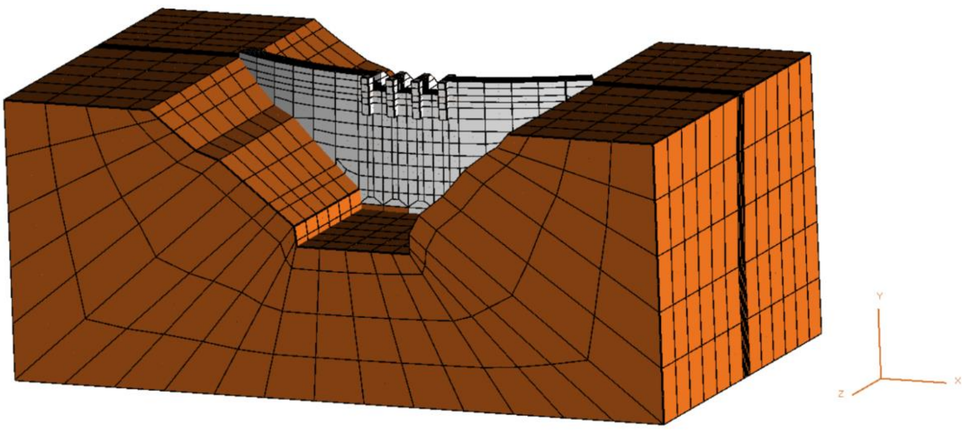

Fig. 4 – Upstream view of the 3D numerical model of Ribeiradio dam

It is assumed that displacements in both the x and y axes shown in Figure 4 are allowed at the upstream and downstream foundation boundaries, as well as displacements in both the y and z axes at the lateral foundation boundaries. The remaining displacements and rotations atthe base of the model and atthe foundation boundaries are prevented.

In the hydraulic model, shown in Figure 5, it is assumed that dam contraction joints are impervious and seepage takes place only along the dam/foundation interface. This interface has 517 hydraulic nodes and 920 hydraulic interfaces, and seepage takes place along 2760 seepage channels. Figure 5 also shows the hydraulic boundary conditions: black hydraulic nodes are impervious areas and blue hydraulic nodes are those where the hydrostatic pressure is imposed, corresponding to the hydrostatic pressure on the upstream and downstream faces of the dam. In this study the grout curtain was not simulated.

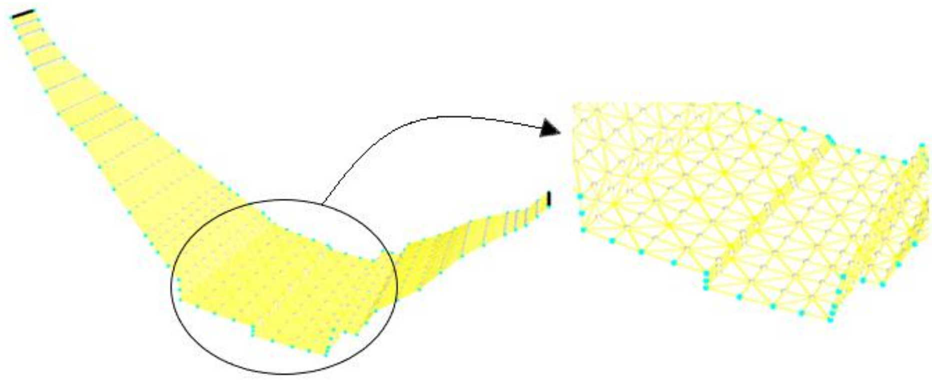

Fig. 5 – Hydraulic interfaces and seepage channels at the dam/foundation interface

Two different situations were analysed, assuming a non-operational drainage system or an operational drainage system. Figure 6 shows two different hypothetical positions of the drainage system, D1 and D2. In reality, the drainage system is located in an intermediate position between D1 and D2.

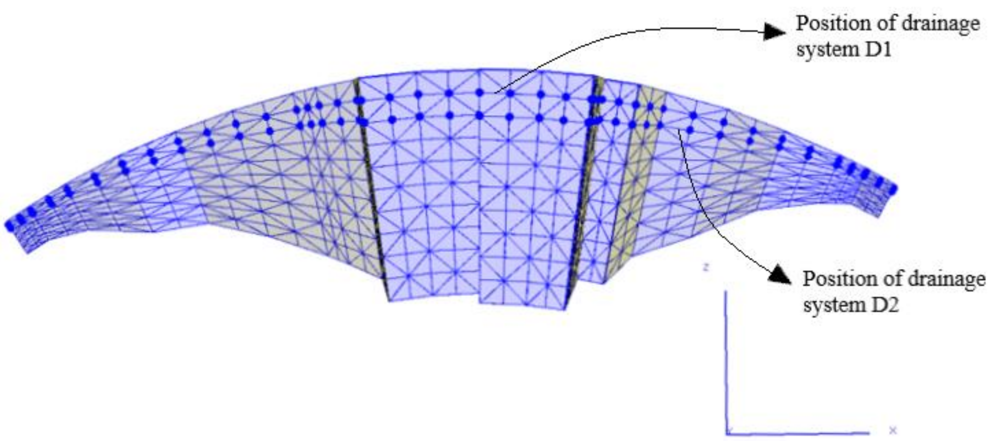

Fig. 6 – View from below of the dam/foundation interface. Two different hypothetical positions of the drainage system (D1 and D2)

3.3. Material properties

Table 1 shows the mechanical properties of both the dam and the foundation and Table 2 shows the mechanical properties of the contraction joints (concrete/concrete) and of the dam/foundation interface. Acceleration due to gravity is assumed to be 10 m/s^2. Regarding the hydraulic properties of the seepage channels, it is assumed that the initial hydraulic aperture ofdiscontinuities, a_0, is equal to0.0834 mm, the minimum aperture, a_{min}, is equal to $a_0/3$ and the maximum aperture, a_{max}, is equal to $5a_{min}$. In this study, a multiplicative factor of $\lambda = 2$ was applied to the seepage channels´ pseudo width.

Table 1 – Mechanical material properties

	Young's modulus E (GPa)	Poisson´s ratio (-)	Density ρ (ton/m^3)	Compressive strength f_c (MPa)	Tensile strength f_{ct} (MPa)
Concrete	20.0	0.2	2.4	20.0	2.0
Rock mass	5.0	0.2	2.7	20.0	2.0

Table 2 – Interface mechanical properties

	Normal stiffness k_n (GPa/m)	Shear stiffness K_s (GPa/m)
Concrete/concrete	40.0	16.0
Dam/foundation	10.0	4.0

3.4. Sequence of analysis

The sequence of analysis includes: i) calculation of in situ stresses due to the weight of the rock mass; ii) consideration of dam weight, and iii) application of hydrostatic loading on the upstream face of the dam and of the uplift at the base of the dam. Finally, sliding stability analysis is carried out, either using the strength reduction method or considering an amplification of the water pressures resulting from an increase of the hydrostatic loading or of the reservoir level.

3.5. Main results

3.5.1 Stresses due to the dam weight

Figure 7 shows the vertical stresses due to the dam weight at the dam upstream and downstream faces. Due to the triangular cross section of the dam, stresses at the upstream face close to the dam/foundation interface are considerably higher than those at the downstream face.

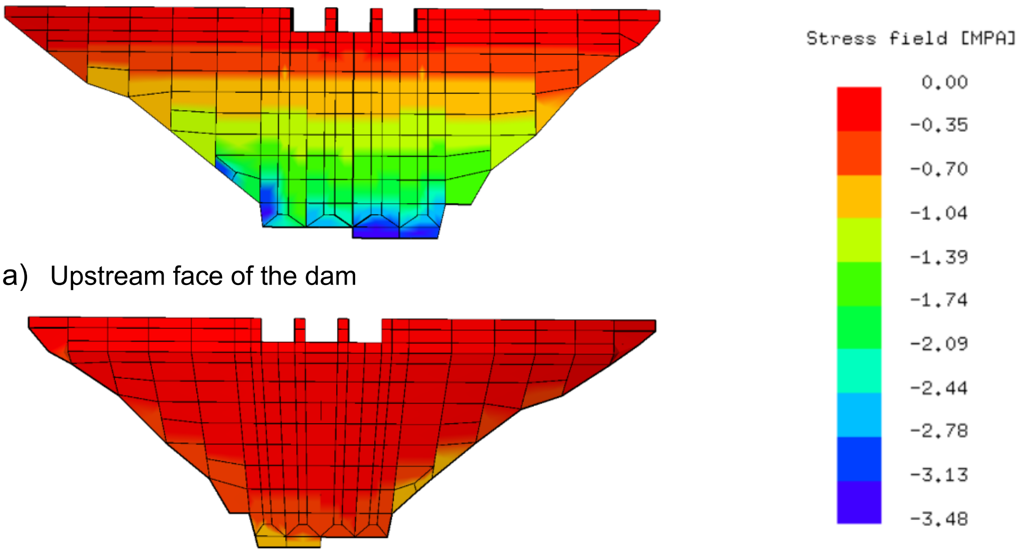

a) Upstream face of the dam

b) Downstream face of the dam

Fig. 7 – Vertical stresses at the dam faces due to dead weight

3.5.2 Water pressures at the base of the dam

Figure 8 shows the distribution of water pressures at the dam/foundation interface calculated with the hydromechanical model. Water pressure varies from 0.83 MPa at the heel of the dam, given from the upstream water level, to zero at the toe of the dam, where the water is assumed to be at the ground level. Observing this figure, it can be concluded that coherent results are obtained both with non-operational and operational drainage systems.

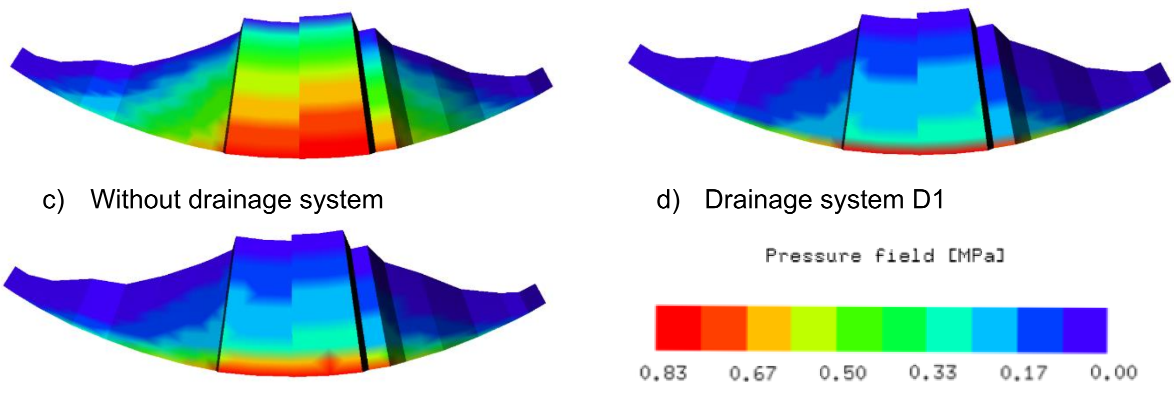

c) Without drainage system

d) Drainage system D1

e) Drainage system D2

Fig. 8 – Water pressures at the base of the dam, calculated with the hydromechanical model

3.5.3 Stresses due to the simultaneous effect of dead weight, hydrostatic pressure and uplift pressure

Figure 9 shows the vertical stresses at the dam upstream and downstream faces due to the simultaneous effect of dead weight, hydrostatic pressure and uplift pressure. Maximum compressive stresses are located, as expected, at the toe of the dam in the valley bottom and have a maximum value of 2.39 MPa.

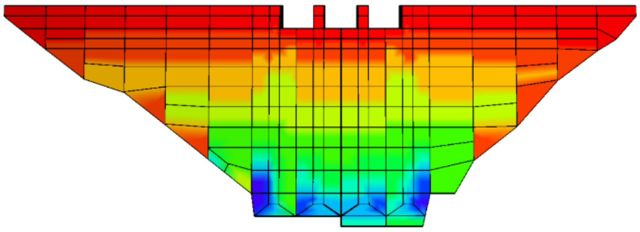

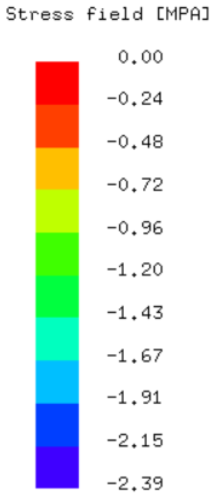

a) Upstream face of the dam

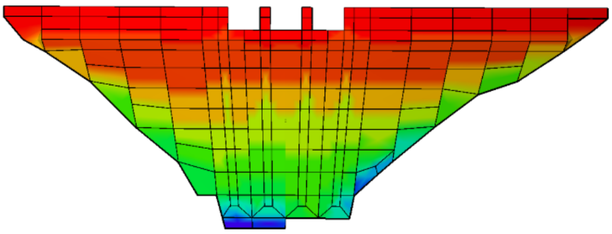

b) Downstream face of the dam

Fig. 9 – Vertical stresses at the dam faces due to the simultaneous effect of dead weight, hydrostatic pressure and uplift pressure

4. STABILITY ANALYSIS

4.1. Models

Analysis of the sliding stability along the dam/foundation interface was carried out using as failure indicator the displacement of the dam crest at the central cantilever. Three different hypotheses were considered, corresponding to the following models:

i) Model A - independent cantilevers assuming only friction at the concrete/concrete interfaces. The hydromechanical analysis is not carried out during the processes of strength reduction at the dam/foundation interface or increase in water loading (uplift pressures remain constant during these processes). In the strength reduction method, only friction is considered at the dam/foundation interface, while in the method of hydrostatic load increase a cohesive brittle contact model is assumed at this interface.

ii) Model B - independent cantilevers assuming only friction at the concrete/concrete interfaces. The hydromechanical analysis is carried out during the processes of strength reduction at the dam/foundation interface or increase in water loading and thus, in this case, uplift pressures change during these processes. In the strength reduction method, only friction is considered at the dam/foundation interface, while in the method of hydrostatic load increase a cohesive brittle contact model is assumed at this interface.

iii) Model C - independent cantilevers assuming only friction at the concrete/concrete interfaces and at the dam/foundation interface. This model is used only when an increase in water pressures is considered and the hydromechanical analysis is carried out during this process.

4.2. Strength reduction method

Safety factors were calculated by progressively diminishing the dam/foundation friction angle until reaching failure (the reduction coefficient was actually applied to the tangent of the friction angle). Cohesion at the dam/foundation interface was assumed to be zero, as prescribed in the Portuguese legislation [14]. Figure 10 shows the variation in dam displacements during the process of reduction of the tangent of the friction angle, considering either a non-operational drainage system (SD) or two different operational drainage systems (D1 or D2).

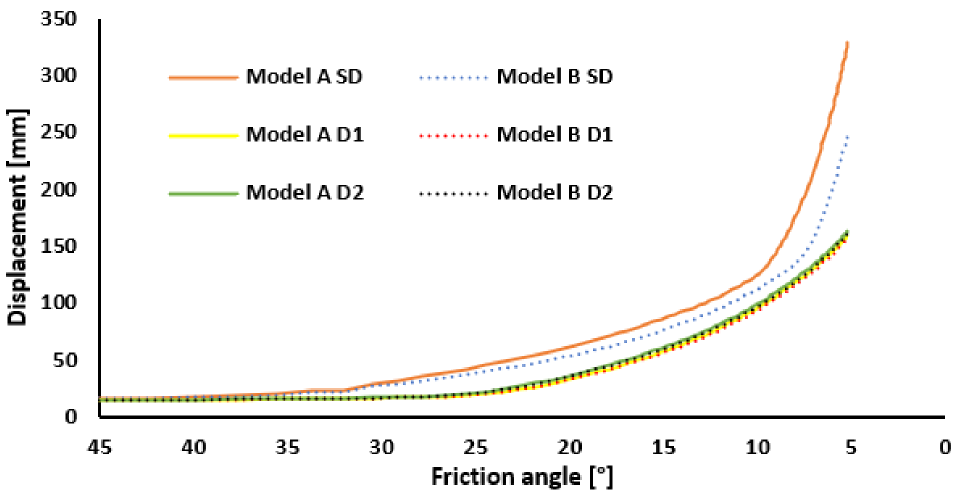

Fig. 10 – Variation in displacements at the top of the central block during the process of friction angle reduction, with non-operational drainage (SD) and with operational drainage (D1 or D2)

With a non-operational drainage system, the safety factor is approximately 1.3, and with operational drainage this factor rises to 1.9 with model A and to 2.0 with model B. Therefore, results obtained when the hydromechanical behaviour is taken into account during the strength reduction analysis (model B) are close to those obtained assuming that the uplift pressure remains constant (model A). These results are also similar to those obtained in another study which assumed a simplified distribution of water pressures at the dam/foundation interface [10].

4.3. Increase in hydrostatic loading

Stability analysis can also be carried out by increasing the water pressure at the upstream face of the dam, using an amplification factor (λ). In hydromechanical coupled analysis, this amplification factor may also influence the uplift pressures (Figure 11). In the numerical simulations carried out, an increment of 0.1 was adopted for λ in each cycle

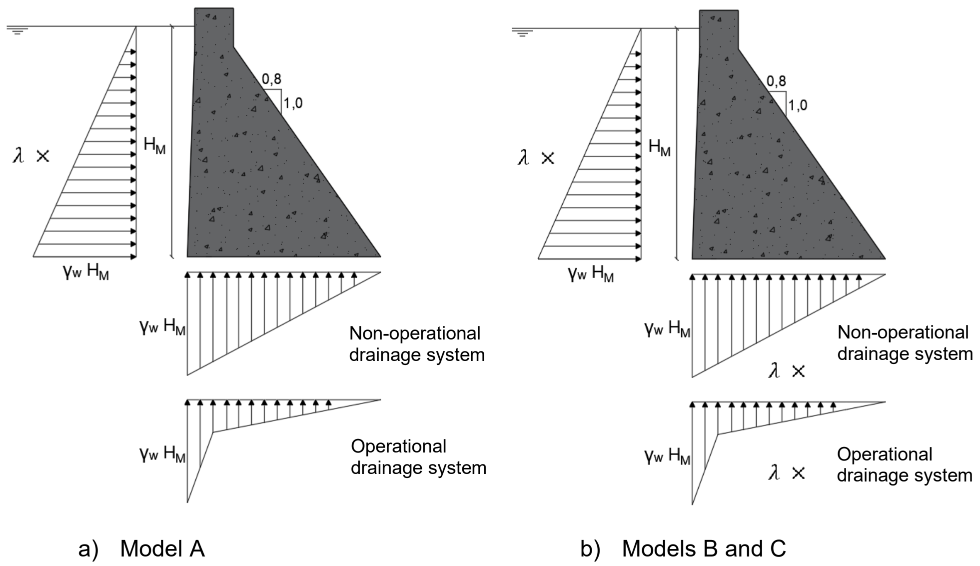

Fig. 11 – Increase in hydrostatic loading using amplification factor λ

Safety factors obtained in the numerical analyses are shown in Table 3. It can be observed that the amplification of the uplift pressures during the process of increasing the hydrostatic pressure leads to significantly lower safety factors.

Table 3 – Safety factors for an increase in hydrostatic loading using an amplification factor

Safety factor								
Model A			Model B			Model C		
SD	D1	D2	SD	D1	D2	SD	D1	D2
4.1	5.5	5.2	1.9	3.1	2.7	1.9	3.1	2.7

4.4. Increase in reservoir level

Another way of performing stability analysis is by increasing the reservoir level, simulating the scenario of dam overtopping.When this approach was followed, an increase of 1.0 m was considered for each cycle. Figure 12 shows qualitatively the influence of this increase of the reservoir level on each model (A, B and C), which obviously depends on the type of hydromechanical analysis (uncoupled or coupled) performed in each model.

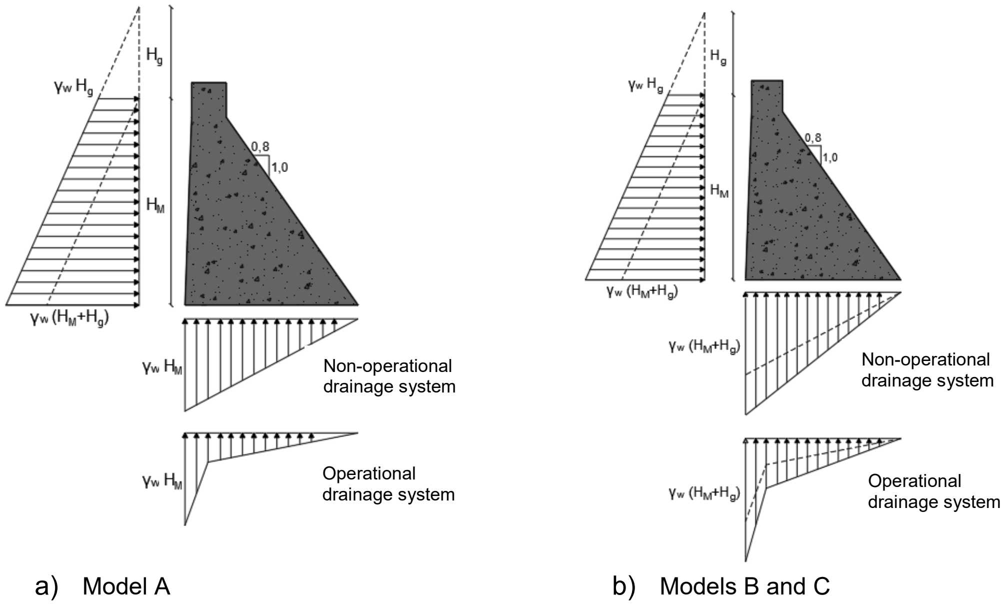

Fig. 12 – Increase of the reservoir level

Safety factors obtained in the numerical analyses for which the reservoir level was gradually increased are shown in Table 4. Comparison of the safety factors presented in Tables 3 and 4 leads to the conclusion that, when the increase in water pressure is due to the rising of the reservoir level, the safety factors are lower than those obtained assuming a direct amplification of the hydrostatic pressure.

Table 4 – Safety factors for an increase of the reservoir level

Safety factor								
Model A			Model B			Model C		
SD	D1	D2	SD	D1	D2	SD	D1	D2
2.30	2.57	2.62	1.85	2.36	2.27	1.88	2.39	2.27

5. CONCLUSIONS

This study presents the results of the 3D hydromechanical analysis of one arch-gravity dam foundation, using an explicit time stepping small displacement algorithm, Parmac3D-Fflow, based on a discrete representation of the discontinuities.

The hydromechanical analysis of the arch-gravity dam foundation highlighted the influence of the drainage system on the distribution of water pressures at the dam/foundation interface. Consistent results are obtained with both non-operational and operational drainage systems. It is also shown that the results obtained when the hydromechanical behaviour is taken into account during the strength reduction analysis are close to those obtained assuming that the uplift pressure remains constant. When the failure scenario of sliding along the dam/foundation interface is studied using the method of increasing the hydrostatic pressure, it is observed that the amplification of the uplift pressures due to the increase of the hydrostatic pressure leads to significantly lower safety factors. When the increase of water pressure is obtained by an increase of the reservoir level, the safety factors are lower than those obtained assuming a direct amplification of the hydrostatic load and closer to those obtained with the strength reduction method.

Advanced numerical analysis is useful to gain a better understanding of the dam foundation hydromechanical behaviour and to assess the dam stability. It is, however, highlighted that the use of these models in real cases requires in situ tests must be carried out, preferably during the dam construction phase, in order to obtain the most adequate parameters to be considered in the numerical analysis. Further work is underway to develop an automatic procedure in order to simulate grout curtains in the foundation of both arch-gravity and arch dams, to improve the validation of the 3D hydromechanical model and to develop parallel algorithms, not only to decrease the computing time but also to make it possible to apply this formulation to more complex and larger geometries.

ACKNOWLEDGMENTS

The study presented here is part of the research project “DAMFA: Cutting-edge solutions for sustainable assessment of concrete dam foundations” which has been supported by LNEC with the main purpose of developing a numerical multiphysic integrated tool for the sustainable assessment of concrete dam foundations, taking into account the interaction between mechanical, hydraulic and thermal behaviours.

REFERENCES

[1] M.L.B. Farinha; J. Lemos; E. Maranha das Neves (2012) Analysis of foundation sliding of an arch dam considering the hydromechanical behaviour. Frontiers of Structural and Civil Engineering 6(1): 35–43.

[2] Schclar Leitão, N.; Castilho, E.; Monteiro Azevedo, N.; Farinha, M.L.B. (2020) Considerations about the use of numerical models in the safety assessment of concrete dams (in Portuguese). Revista Portuguesa de Engenharia de Estruturas III (12): 5-16.

[3] Lombardi, G. (2007). 3-D analysis of gravity dams. The International Journal of Hydropower and Dams 14(1): pp. 98-102.

[4] Lemos, J.V. (2011). Discontinuum models for dam foundation failure analysis. Keynote Lecture, 12th International Congress on Rock Mechanics, Beijing, China, 16-21 October 2011.

[5] M.L.B. Farinha; J. Lemos; E. Maranha das Neves (2011) Numerical modelling of borehole water inflow tests in the foundation of the Alqueva arch dam, Canadian Geotechnical Journal 48(1): 72-88.

[6] Monteiro Azevedo, N., Farinha, M.L.B. (2015). A hydromechanical model for the analysis of concrete gravity dam foundations (in Portuguese). Geotecnia, Volume 133 (março): 5-33.

[7] Farinha, M.L.B.; Monteiro Azevedo, N.; Candeias, M. (2017). Small displacement coupled analysis of concrete gravity dam foundations: static and dynamic conditions. Rock Mechanics Rock Engineering 50(2): 439-464.

[8] Farinha, M.L.B.; Monteiro Azevedo, N.; Schclar Leitão, N.; Castilho, E.; Câmara, R. (2018) 3D coupled hydromechanical analysis of dam foundations. Proceedings of the 9th European Conference on Numerical Methods in Geotechnical Engineering NUMGE18, FEUP, Porto, 25-27 June 2018: 1241-1248.

[9] Sá, M.W.V. (2019). Discontinuum models in the three-dimensional analysis of the hydromechanical behaviour of gravity dam foundations (in Portuguese). MSc Dissertation, Faculdade de Ciências e Tecnologia da Universidade Nova de Lisboa, Portugal.

[10] Gomes, M.E.A. (2019). Discrete crack models in the sliding stability analysis of an arch-gravity dam (In Portuguese). MSc Dissertation, Faculdade de Ciências e Tecnologia da Universidade Nova de Lisboa, Portugal.

[11] Monteiro Azevedo N. (2003). A rigid particle discrete element model for the fracture analysis of plane and reinforced concrete. PhD Dissertation, Heriot-Watt University, Scotland.

[12] Yan, C.; Zheng, H. (2017). FDEM-flow3D: A 3D hydro-mechanical coupled model considering the pore seepage of rock matrix for simulating three-dimensional hydraulic fracturing. Computers and Geotechnics 81: 212-228.

[13] Oliveira, S.; Silvestre, A.; Câmara, R. (2014). Barragem de Ribeiradio. Verificação da segurança estrutural para ações estáticas e dinâmicas. Relatório LNEC 419/2014 - DDB/NMMR.

[14] RSB (2018). Regulamento de Segurança de Barragens. Diário da República. Decreto-Lei n.º 21/2018 de 28 de março